3

Incompressible Non-Newtonian Fluid Flows

Quoc-Hung Nguyen and Ngoc-Diep Nguyen
Mechanical Faculty, Ho Chi Minh University of Industry,
Vietnam

1. Introduction

A non-Newtonian fluid is a fluid whose flow properties differ in many ways from those of Newtonian fluids. Most commonly the viscosity of non-Newtonian fluids is not independent of shear rate or shear rate history. In practice, many fluid materials exhibits non-Newtonian fluid behavior such as: salt solutions, molten, ketchup, custard, toothpaste, starch suspensions, paint, blood, and shampoo etc. In a Newtonian fluid, the relation between the shear stress and the shear rate is linear, passing through the origin, the constant of proportionality being the coefficient of viscosity. In a non-Newtonian fluid, the relation between the shear stress and the shear rate is different, and can even be time-dependent. Therefore a constant coefficient of viscosity cannot be defined. In the previous parts of this book, the mechanics of Newtonian fluid have been mentioned. In this chapter, the common rheological models of non-Newtonian fluids are introduced and several approaches concerned with non-Newtonian fluid flows are considered. In addition, the solution of common non-Newtonian fluid flows in a circular pipe, annular and rectangular duct are presented.

2. Classification of non-Newtonian fluid

As above mentioned, a non-Newtonian fluid is one whose flow curve (shear stress versus shear rate) is nonlinear or does not pass through the origin, i.e. where the apparent viscosity, shear stress divided by shear rate, is not constant at a given temperature and pressure but is dependent on flow conditions such as flow geometry, shear rate, etc. and sometimes even on the kinematic history of the fluid element under consideration. Such materials may be conveniently grouped into three general classes:

1. fluids for which the rate of shear at any point is determined only by the value of the shear stress at that point at that instant; these fluids are variously known as 'time independent' , ' purely viscous' , 'inelastic' or 'generalized Newtonian fluids');
2. more complex fluids for which the relation between shear stress and shear rate depends, in addition, upon the duration of shearing and their kinematic history; they are called 'time-dependent fluids', and finally,
3. substances exhibiting characteristics of both ideal fluids and elastic solids and showing partial elastic recovery, after deformation; these are categorized as 'viscoplastic fluids'.

Among the three groups, the time independent Non-Newtonian fluids are the most popular and easiest to handle in analysis. In this chapter, only this group of Non-Newtonian fluids are considered.
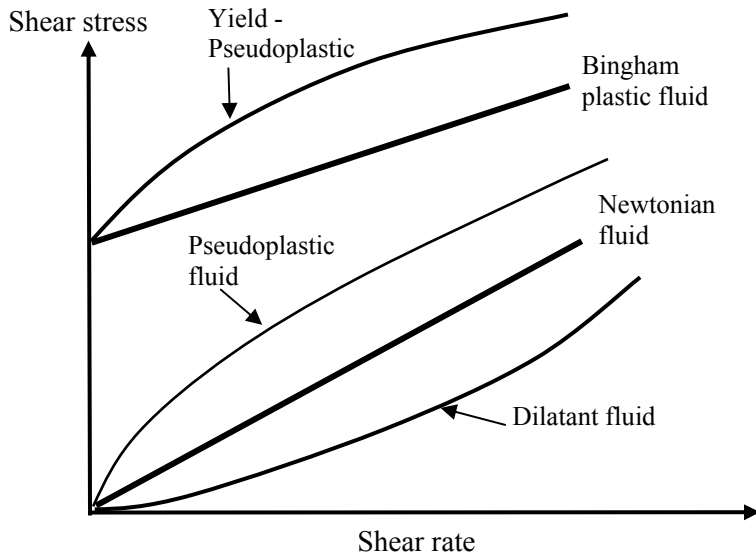
Fig. 1. Types of time-independent non-Newtonian fluid

In simple shear, the flow behaviour of this class of materials may be described by the following constitutive relation,

$$\tau_{yx} = f(\dot{\gamma}_{yx}) \tag{1}$$

This equation implies that the value of $\dot{\gamma}_{yx}$ at any point within the sheared fluid is determined only by the current value of shear stress at that point or vice versa. Depending upon the form of the function in equation (1), these fluids may be further subdivided into three types: shear-thinning or pseudoplastic, shear-thickening or dilatant and viscoplastic

2.1 Shear-thinning or pseudo-plastic fluids

The most common type of time-independent non-Newtonian fluid behaviour observed is Pseudo-plasticity or shear-thinning, characterized by an apparent viscosity which decreases with increasing shear rate. Both at very low and at very high shear rates, most shear-thinning polymer solutions and melts exhibit Newtonian behaviour, i.e., shear stress–shear rate plots become straight lines and on a linear scale will pass through origin. The resulting values of the apparent viscosity at very low and high shear rates are known as the zero shear viscosity, μ_0 , and the infinite shear viscosity, μ_∞, respectively. Thus, the apparent viscosity of a shear-thinning fluid decreases from μ_0 to μ_∞ with increasing shear rate. Many mathematical expressions of varying complexity and form have been proposed in the literature to model shear-thinning characteristics; some of these are straightforward attempts at curve fitting, giving empirical relationships for the shear stress (or apparent viscosity)–shear rate curves for example, while others have some theoretical basis in statistical mechanics – as an extension of the application of the kinetic theory to the liquid state or the theory of rate processes, etc. Only a selection of the more widely used viscosity

models is given here; more complete descriptions of such models are available in many books (Bird *et al* ., 1987 ; Carreau *et al* ., 1997) and in a review paper (Bird, 1976).

i.   The power-law model

The relationship between shear stress and shear rate for this type of fluid can be mathematically expressed as follows:

$$\tau_{yx} = K(\dot{\gamma}_{yx})^n \tag{2}$$

So the apparent viscosity for the so-called power-law fluid is thus given by:

$$\mu = K(\dot{\gamma}_{yx})^{n-1} \tag{3}$$

For $n < 1$, the fluid exhibits shear-thinning properties
          $n = 1$, the fluid shows Newtonian behaviour
          $n > 1$, the fluid shows shear-thickening behaviour

In these equations, K and n are two empirical curve-fitting parameters and are known as the fluid consistency coefficient and the flow behaviour index respectively. For a shear thinning fluid, the index may have any value between 0 and 1. The smaller the value of n, the greater is the degree of shear-thinning. For a shear-thickening fluid, the index n will be greater than unity. When $n=1$, equations (3) becomes the constitutive equation of Newtonian fluid.

Although the power-law model offers the simplest representation of shear-thinning behaviour, it does have a number of limitations. Generally, it applies over only a limited range of shear rates and therefore the fitted values of K and n will depend on the range of shear rates considered. Furthermore, it does not predict the zero and infinite shear viscosities. Finally, it should be noted that the dimensions of the flow consistency coefficient, K, depend on the numerical value of n and therefore the K values must not be compared when the n values differ. On the other hand, the value of K can be viewed as the value of apparent viscosity at the shear rate of unity and will therefore depend on the time unit (e.g. second, minute or hour) employed. Despite these limitations, this is perhaps the most widely used model in the literature dealing with process engineering applications. Table 1 provides a compilation of the power-law constants (K and n) for a variety of substances.

ii.   The Carreau viscosity equation

When there are significant deviations from the power-law model at very high and very low shear rates, it is necessary to use a model which takes account of the limiting values of viscosities μ_0 and μ_∞ . Based on the molecular network considerations, Carreau (1972) put forward the following viscosity model.

$$\frac{\mu - \mu_\infty}{\mu_0 - \mu_\infty} = [1 + (\lambda \dot{\gamma}_{yx})^2]^{(n-1)/2} \tag{4}$$

where n (< 1) and λ are two curve-fitting parameters. This model can describe shear thinning behaviour over wide ranges of shear rates but only at the expense of the added complexity of four parameters. This model predicts Newtonian fluid behaviour $\mu = \mu_0$ when either $n = 1$ or $\lambda =0$ or both.

System	Temperature (K)	n	M (Pa s^n)
Agro- and food-related products			
Ammonium alginate solution (3.37%)	297	0.5	13
Apple butter	–	0.15	200
Apple sauce	300	0.3–0.45	12–22
Apricot puree	300	0.3–0.4	5–20
Banana puree	293–315	0.33–0.5	4–10
Carrot puree	298	0.25	25
Chicken (minced)	296	0.10	900
Chocolate	303	0.5	0.7
Guava puree	296.5	0.5	40
Human blood	300	0.9	0.004
Mango pulp	300–340	0.3	3–10
Marshmallow cream	–	0.4	560
Mayonnaise	298	0.6	5–100
Papaya puree	300	0.5	10
Peach puree	300	0.38	1–5
Peanut butter	–	0.07	500
Pear puree	300	0.4–0.5	1–5
Plum puree	287	0.35	30–80
Tomato concentrate (5.8% solid)	305	0.6	0.22
Tomato ketchup	295	0.24	33
Tomato paste	–	0.5	15
Whipped desert toppings	–	0.12	400
Yoghurt	293	0.5–0.6	25
Polymer melts			
High density polyethylene (HDPE)	453–493	0.6	$3.75–6.2 \times 10^3$
High impact polystyrene	443–483	0.20	$3.5–7.5 \times 10^4$
Polystyrene	463–498	0.25	$1.5–4.5 \times 10^4$
Polypropylene	453–473	0.40	$4.5–7 \times 10^3$
Low density polyethylene (LDPE)	433–473	0.45	$4.3–9.4 \times 10^3$
Nylon	493–508	0.65	$1.8–2.6 \times 10^3$
Polymethylmethyacrylate (PMMA)	493–533	0.25	$2.5–9 \times 10^4$
Polycarbonate	553–593	0.65–0.8	$1–8.5 \times 10^3$
Personal care products			
Nail polish	298	0.86	750
Mascara	298	0.24	200
Toothpaste	298	0.28	120
Sunscreen lotions	298	0.28	75
Ponds cold cream	298	0.45	25
Oil of Olay	298	0.22	25

Source: Modified after Johnson (1999)

Table 1. Typical values of power-law constants for a few systems

iii. The Cross viscosity equation

Another four parameter model which has gained wide acceptance is due to Cross (1965) which, in simple shear, is written as:

$$\frac{\mu - \mu_\infty}{\mu_0 - \mu_\infty} = \frac{1}{1 + k(\dot{\gamma}_{yx})^n} \tag{5}$$

Here n (<1) and k are two fitting parameters whereas μ_0 and μ_∞ are the limiting values of the apparent viscosity at low and high shear rates, respectively. This model reduces to the Newtonian fluid behaviour as $k \rightarrow 0$. Similarly, when $\mu << \mu_0$ and $\mu >> \mu_\infty$, it reduces to the familiar power-law model, equation (3). Though initially Cross (1965) suggested that a constant value of $n = 2/3$ was adequate to approximate the viscosity data for many systems, it is now thought that treating the index, n, as an adjustable parameter offers considerable improvement over the use of the constant value of n (Barnes *et al.*, 1989).

iv. The Ellis fluid model

When the deviations from the power-law model are significant only at low shear rates, it is more appropriate to use the Ellis model. The three viscosity equations presented so far are examples of the form of equation (1). The three-constant Ellis model is an illustration of the inverse form. In simple shear, the apparent viscosity of an Ellis model fluid is given by:

$$\mu = \frac{\mu_0}{1 + (\tau_{yx} / \tau_{1/2})^{\alpha - 1}} \tag{6}$$

In this equation, μ_0 is the zero shear viscosity and the remaining two constants α (> 1) and $\tau_{1/2}$ are adjustable parameters. While the index α is a measure of the degree of shear thinning behaviour (the greater the value of α, greater is the extent of shear-thinning), $\tau_{1/2}$ represents the value of shear stress at which the apparent viscosity has dropped to half its zero shear value. Equation (6) predicts Newtonian fluid behaviour in the limit of $\tau_{1/2} \rightarrow \infty$. This form of equation has advantages in permitting easy calculation of velocity profiles from a known stress distribution, but renders the reverse operation tedious and cumbersome. It can easily be seen that in the intermediate range of shear stress (or shear rate), $(\tau_{yx} / \tau_{1/2})^{\alpha-1} >> 1$, and equation (6) reduces to equation (3) with $n = (1/\alpha)$ and $m = (\mu_0 \tau_{1/2}^{\alpha-1})^{1/\alpha}$

2.2 Viscoplastic fluid behaviour

This type of fluid behaviour is characterized by the existence of a yield stress (τ_0) which must be exceeded before the fluid will deform or flow. Conversely, such a material will deform elastically (or flow *en masse* like a rigid body) when the externally applied stress is smaller than the yield stress. Once the magnitude of the external stress has exceeded the value of the yield stress, the flow curve may be linear or non-linear but will not pass through origin (Figure 1). Hence, in the absence of surface tension effects, such a material

will not level out under gravity to form an absolutely flat free surface. One can, however, explain this kind of fluid behaviour by postulating that the substance at rest consists of three-dimensional structures of sufficient rigidity to resist any external stress less than τ_0. For stress levels greater than τ_0, however, the structure breaks down and the substance behaves like a viscous material. In some cases, the build-up and breakdown of structure has been found to be reversible, i.e., the substance may regain its initial value of the yield stress.

A fluid with a linear flow curve for $|\tau_{yx}| > |\tau_0|$ is called a Bingham plastic fluid and is characterized by a constant plastic viscosity (the slope of the shear stress versus shear rate curve) and a yield stress. On the other hand, a substance possessing a yield stress as well as a non-linear flow curve on linear coordinates (for $|\tau_{yx}| > |\tau_0|$), is called a yield pseudoplastic material. It is interesting to note that a viscoplastic material also displays an apparent viscosity which decreases with increasing shear rate. At very low shear rates, the apparent viscosity is effectively infinite at the instant immediately before the substance yields and begins to flow. It is thus possible to regard these materials as possessing a particular class of shear-thinning behaviour.

Strictly speaking, it is virtually impossible to ascertain whether any real material has a true yield stress or not, but nevertheless the concept of a yield stress has proved to be convenient in practice because some materials closely approximate to this type of flow behaviour, e.g. see Barnes and Walters (1985) , Astarita (1990) , Schurz (1990) and Evans (1992) . Many workers in this field view the yield stress in terms of the transition from a solid-like (high viscosity) to a liquid-like (low viscosity) state which occurs abruptly over an extremely narrow range of shear rates or shear stress (Uhlherr *et al* ., 2005). It is not uncommon for the two values of viscosity to differ from each other by several orders of magnitude. The answer to the question whether a fluid has a yield stress or not seems to be related to the choice of a time scale of observation. Common examples of viscoplastic fluid behaviour include particulate suspensions, emulsions, foodstuffs, blood and drilling mud, etc. (Barnes, 1999).

Over the years, many empirical expressions have been proposed as a result of straightforward curve-fitting exercises. A model based on sound theory is yet to emerge. Three commonly used models for viscoplastic fluids are: Bingham plastic model, Herschel-Bulkley model and Casson model.

i.   The Bingham plastic model

This is the simplest equation describing the flow behaviour of a fluid with a yield stress and, in steady one-dimensional shear, it is described by

$$\tau_{yx} = \tau_0 + \mu(\dot{\gamma}_{yx}) \ \text{ for } \left|\tau_{yx}\right| > \left|\tau_0\right|$$

$$\dot{\gamma}_{yx} = 0 \ \text{ for } \left|\tau_{yx}\right| < \left|\tau_0\right| \hspace{3cm} (7)$$

Often, the two model parameters τ_0 and μ are treated as curve-fitting constants irrespective of whether or not the fluid possesses a true yield stress.

ii. The Herschel-Bulkley fluid model

A simple generalization of the Bingham plastic model to embrace the non-linear flow curve (for $\tau_{yx} > \tau_0$) is the three constant Herschel–Bulkley fluid model. In one dimensional steady shearing motion, the model is written as:

$$\tau_{yx} = \tau_0 + K(\dot{\gamma}_{yx})^n \ \text{ for } \ |\tau_{yx}| > |\tau_0|$$

$$\dot{\gamma}_{yx} = 0 \ \text{ for } \ |\tau_{yx}| < |\tau_0| \tag{8}$$

It is again noted that, the dimensions of K depend upon the value of n. With the use of the third parameter, this model provides a somewhat better fit to some experimental data.

iii. The Casson fluid model

Many foodstuffs and biological materials, especially blood, are well described by this two constant model as:

$$|\tau_{yx}|^{1/2} = |\tau_0|^{1/2} + (\mu / \dot{\gamma}_{yx})^{1/2} \ \text{ for } \ |\tau_{yx}| > |\tau_0|$$

$$\dot{\gamma}_{yx} = 0 \ \text{ for } \ |\tau_{yx}| < |\tau_0| \tag{9}$$

This model has often been used for describing the steady shear stress–shear rate behaviour of blood, yoghurt, tomato purée, molten chocolate, etc. The flow behaviour of some particulate suspensions also closely approximates to this type of behaviour. The comparative performance of these three as well as several other models for viscoplastic behaviour has been thoroughly evaluated in an extensive review paper by Bird *et al* . (1983) and a through discussion on the existence, measurement and implications of yield stress has been provided by Barnes (1999).

2.3 Shear-thickening or dilatant fluid behaviour

Dilatant fluids are similar to pseudoplastic systems in that they show no yield stress but their apparent viscosity increases with increasing shear rate; thus these fluids are also called shear-thickening. This type of fluid behaviour was originally observed in concentrated suspensions and a possible explanation for their dilatant behaviour is as follows: At rest, the voidage is minimum and the liquid present is sufficient to fill the void space. At low shear rates, the liquid lubricates the motion of each particle past others and the resulting stresses are consequently small. At high shear rates, on the other hand, the material expands or dilates slightly (as also observed in the transport of sand dunes) so that there is no longer sufficient liquid to fill the increased void space and prevent direct solid–solid contacts which result in increased friction and higher shear stresses. This mechanism causes the apparent viscosity to rise rapidly with increasing rate of shear. The term dilatant has also been used for all other fluids which exhibit increasing apparent viscosity with increasing rate of shear. Many of these, such as starch pastes, are not true suspensions and show no dilation on shearing. The above explanation therefore is not applicable but nevertheless such materials are still commonly referred to as dilatant fluids.

Of the time-independent fluids, this sub-class has received very little attention; consequently very few reliable data are available. Until recently, dilatant fluid behaviour was considered to be much less widespread in the chemical and processing industries. However, with the recent growing interest in the handling and processing of systems with high solids loadings, it is no longer so, as is evidenced by the number of recent review articles on this subject (Barnes *et al*., 1987; Barnes, 1989; Goddard and Bashir, 1990). Typical examples of materials exhibiting dilatant behaviour include concentrated suspensions of china clay, titanium dioxide (Metzner and Whitlock, 1958) and of corn fl our in water (Griskey *et al*., 1985). The limited information reported so far suggests that the apparent viscosity–shear rate data often result in linear plots on double logarithmic coordinates over a limited shear rate range and the flow behaviour may be represented by the power-law model, with the flow behaviour index, *n*, greater than unity, i.e.,

$$\mu = K(\dot{\gamma}_{xy})^{n-1} \qquad\qquad (10)$$

One can readily see that for *n* > 1, equation (10) predicts increasing viscosity with increasing shear rate. The dilatant behaviour may be observed in moderately concentrated suspensions at high shear rates, and yet, the same suspension may exhibit pseudoplastic behaviour at lower shear rates.

This section is concluded by Table 2 providing a list of materials displaying a spectrum of non-Newtonian flow characteristics in diverse applications to reinforce idea yet again of the ubiquitous nature of such flow behaviour.

Practical fluid	Characteristics	Consequence of non-Newtonian behaviour
Toothpaste	Bingham Plastic	Stays on brush and behaves more liquid-like while brushing
Drilling muds	Bingham Plastic	Good lubrication properties and ability to convey debris
Non-drip paints	Thixotropic	Thick in the tin, thin on the brush
Wallpaper paste	Pseudoplastic and Viscoelastic	Good spreadability and adhesive properties
Egg white	Visco-elastic	Easy air dispersion (whipping)
Molten polymers	Visco-elastic	Thread-forming properties
' Bouncing Putty '	Visco-elastic	Will flow if stretched slowly, but will bounce (or shatter) if hit sharply
Wet cement aggregates	Dilatant and thixotropic	Permit tamping operations in which small impulses produce almost complete settlement
Printing inks	Pseudoplastic	Spread easily in high speed machines yet do not run excessively at low speeds
Waxy crude oils	Viscoplastic and Thixotropic	Flows readily in a pipe, but difficult to restart the flow

Table 2. Non-Newtonian characteristics of some common materials

3. Rabinowitsch-Mooney equation

Consider a one-directional flow of fluid through a circular tube with radius R, Figure 2. The volumetric flow rate through an annular element of area perpendicular to the flow and of width δr is given by

$$\delta Q \;=\; 2\pi r \delta r.v_x \tag{11}$$

and, consequently, the flow rate through the whole tube is

$$Q \;=\; 2\pi \int_0^R r v_x dr \tag{12}$$

Integrating by parts gives

$$Q \;=\; 2\pi \left\{ \left[\frac{r^2 v_x}{2} \right]_0^{r_i} + \int_0^{r_i} \frac{r^2}{2}\left(-\frac{dv_x}{dr} \right)dr \right\} \tag{13}$$

Provided there is no slip at the tube wall, the first term in equation (13) vanishes. Equation (13) then can be written as

$$Q \;=\; \pi \int_0^R r^2 (-\dot{\gamma})dr \tag{14}$$

If the fluid is time-independent and homogeneous, the shear stress is a function of shear rate only. The inverse is that the shear rate $\dot{\gamma}$, is a function of shear stress τ_{rx} only and the variation of τ_{rx} with r is known from the following well-known equation:

$$\frac{\tau_{rx}}{\tau_w} \;=\; \frac{r}{R} \tag{15}$$

where τ_w is the wall shear stress.

Changing variables in equation (14), using equation (15), and dropping the subscripts rx, equation (14) can be written as

$$Q \;=\; \pi \int_0^{\tau_w} \frac{\tau^2 R^2}{\tau_w^2} (-\dot{\gamma}) \frac{\tau_i}{\tau_w} d\tau \;=\; \frac{\tau R^3}{\tau_w^3} \int_0^{\tau_w} \tau^2 (-\dot{\gamma}) d\tau \tag{16}$$

where $\dot{\gamma}$ is interpreted as a function of τ instead of r.
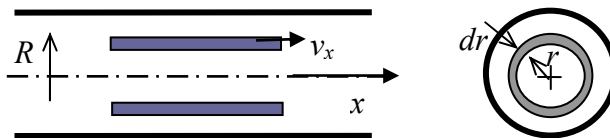
Fig. 2. Geometric presentation of MR fluid in o circular tube

Writing equation (16) in terms of the flow characteristic gives

$$\frac{8u}{D} = \frac{4Q}{\pi R^3} = \frac{4}{\tau_w^3} \int_0^{\tau_w} \tau^2(-\dot{\gamma}) d\tau \tag{17}$$

where u is the average velocity of the fluid flow and D is the diameter of the tube. For flow in a pipe or tube the shear rate is negative so the integral in equation (17) is positive. For a given relationship between τ and $\dot{\gamma}$, the value of the integral depends only on the value of τ_w. Thus, for a non-Newtonian fluid, as well as for a Newtonian fluid, the flow characteristic $8u/D$ is a unique function of the wall shear stress τ_w.

The shear rate $\dot{\gamma}$ can be extracted from equation (17) by differentiating with respect to τ. Moreover, if a definite integral is differentiated w.r.t. the upper limit (τ_w), the result is the integrand evaluated at the upper limit. It is convenient first to multiply equation (17) by τ_w^3 throughout, then differentiating w.r.t. τ_w gives

$$3\tau_w^2 \frac{8u}{D} + \tau_w^3 \frac{d(8u/D)}{d\tau_w} = 4\tau_w^2(-\dot{\gamma})_w \tag{18}$$

Rearranging equation (18) gives the wall shear rate $\dot{\gamma}_w$ as

$$-\dot{\gamma}_w = \frac{8u}{D}\left[\frac{3}{4} + \frac{1}{4}\frac{\tau_w}{(8u/D)}\frac{d(8u/D)}{d\tau_w}\right] \tag{19}$$

Making use of the relationship $dx/x = dlnx$, equation (19) can be written as

$$-\dot{\gamma}_w = \frac{8u}{D}\left[\frac{3}{4} + \frac{1}{4}\frac{d\ln(8u/D)}{d\ln\tau_w}\right] \tag{20}$$

As the wall shear rate $\dot{\gamma}_{wN}$ for a Newtonian fluid in laminar flow is equal to (-8u/D), equation (20) can be expressed as

$$\dot{\gamma}_w = \dot{\gamma}_{wN}\left[\frac{3}{4} + \frac{1}{4}\frac{d\ln(8u/D)}{d\ln\tau_w}\right] \tag{21}$$

Equations (20) and (21) are forms of the Rabinowitsch-Mooney equation. It shows that the wall shear rate for a non-Newtonian fluid can be calculated from the value for a Newtonian fluid having the same flow rate in the same pipe, the correction factor being the quantity in the square brackets. The derivative can be estimated by plotting $ln(8u/D)$ against $\ln\tau_w$ and measuring the gradient. Alternatively the gradient may be calculated from the (finite) differences between values of $ln(8du/D)$ and $\ln\tau_w$. Thus the flow curve τ_w against $\dot{\gamma}_w$ can be determined. The measurements required and the calculation procedure are as follows.

1. Measure Q at various values of $\Delta P_f / L$, preferably eliminating end effects.
2. Calculate τ_ω from the pressure drop measurements and the corresponding values of the flow characteristic $(8du/D = 4Q/\pi R^3)$ from the flow rate measurements.

3. Plot $\ln(8du/D)$ against $\ln\tau_w$ and measure the gradient at various points on the curve. Alternatively, calculate the gradient from the differences between the successive values of these quantities.
4. Calculate the true wall shear rate from equation (20) with the derivative determined in step 3. In general, the plot of $\ln(8du/D)$ against $\ln\tau_w$ will not be a straight line and the gradient must be evaluated at the appropriate points on the curve.

Example 1

The flow rate-pressure drop measurements shown in Table 3 were made in a horizontal tube having an internal diameter D = 6 mm, the pressure drop being measured between two tapings 2.0m apart. The density of the fluid, ρ, was 870 kg/m³. Determine the wall shear stress-flow characteristic curve and the shear stress-true shear rate curve for this material.

Pressure drop (bar)	Mass flow rate x 10³ (kg/s)
0.384	0.0864
0.519	0.463
0.716	1.37
0.965	2.76
1.16	4.13
1.29	5.20
1.46	6.78
1.60	8.15

Table 3.

The results are shown in Table 4

τ_ω (Pa)	$8du/D$	gradient n'	$(3n'+1)/4n'$	$-\dot\gamma_\omega(\text{s}^{-1})$
28.8	4.68	0.157	2.34	11.0
38.9	25.1	0.232	1.83	45.9
53.7	74.3	0.375	1.42	106
72.4	150	0.439	1.32	197
87.0	224	0.475	1.28	286
96.8	282	0.475	1.28	360
110	367	0.475	1.28	469
120	442	0.475	1.28	564

Table 4

4. Calculation of flow rate-pressure drop relationship for laminar flow using $\tau-\dot\gamma$ data

Flow rate-pressure drop calculations for laminar non-Newtonian flow in pipes may be made in various ways depending on the type of flow information available. When the flow data are in the form of flow rate and pressure gradient measured in a tubular viscometer or in a

pilot scale pipeline, direct scale-up can be done as described in Section 5. When the data are in the form of shear stress-shear rate values (tabular or graphical), the flow rate can be calculated directly using equation (17), where D is the diameter of the pipe to be used and τ_w is the wall shear stress corresponding to the specified pressure gradient. Whether obtained with a rotational instrument or with a tubular viscometer, the data provide the relationship between τ and $\dot{\gamma}$. Numerical evaluation of the integral in equation (17) can be done using selected pairs of values of τ and $\dot{\gamma}$ ranging from 0 to τ_w.

If the $\tau - \dot{\gamma}$, relationship can be accurately represented by a simple algebraic expression, such as the power law, over the required range then this may be used to substitute for $\dot{\gamma}$, in equation (17), allowing the integral to be evaluated analytically. Both these methods are illustrated in the following example.

Example 2

Using the viscometric data given in Table 5 calculate the average velocity for the material flowing through a pipe of diameter 37mm when the pressure gradient is 1.1kPa/m.

$\dot{\gamma}(s^{-1})$	τ (Pa)	μ_a $(Pa\ s)$
0.00911	0.0417	4.58
0.0911	0.175	1.95
0.911	0.708	0.777
9.111	2.82	0.310
91.11	11.22	0.123
102.3	12.03	0.118

Table 5.

Calculations

The wall shear stress is given by

$$\tau_w \;=\; \frac{D\Delta P}{4L} \;=\; \frac{(37 \times 10^{-3}\mathrm{m})(1100\ \mathrm{Pa/m})}{4} \;=\; 10.18\ \mathrm{Pa}$$

the flow characteristic

$$\frac{8u}{D} \;=\; \frac{4}{\tau_w^3}\int_0^{\tau_w} \tau^2(-\dot{\gamma})d\tau$$

It is necessary to evaluate the integral from τ = 0 to τ = 10.18Pa. This can be done by calculating $\tau^2\dot{\gamma}$ for each of the values given in the table and plotting $\tau^2\dot{\gamma}$ against τ. The area under the curve between τ = 0 and τ = 10.18Pa can then be measured. An alternative, which will be used here, is to use a numerical method such as Simpson's rule. This requires values at equal intervals of τ. Dividing the range of integration into six strips and interpolating the data allows Table 6 to be constructed.

τ (Pa)	$\dot{\gamma}$	$\tau^2 \dot{\gamma}$
0.00	0.0	0.00 (Centerline)
1.70	3.91	11.24
3.39	12.41	142.8
5.09	24.38	631.0
6.78	39.39	1812
8.48	57.14	4108
10.18	77.43	8016 (pipe wall)

Table 6.

By Simpson's rule

$$\int_0^{10.18} \tau^2 \dot{\gamma} d\tau \approx \frac{10.18/6}{3}[0+8016+4(11.24+613+4108)+2(142.8+1812)]= \ 17490 \ \text{Pa}^3\text{s}^{-1}$$

From equation (17)

$$u = \frac{(37 \times 10^{-3}\text{m})(17490 \ \text{Pa}^3\text{s}^{-1})}{2(10.18 \ \text{Pa})^3} \ = 0.307 \ \text{m/s}$$

The above is the general method but in this case the viscometric data can be well represented by $\tau = 0.749\dot{\gamma}^{0.60} \ Pa$, thus $\dot{\gamma} = 1.62\tau^{1.667} \ s^{-1}$. This allows the integral in equation (17) to be evaluated analytically.

$$\int_0^{\tau_\omega} \tau^2 \dot{\gamma} d\tau = 1.62 \int_0^{10.18} \tau^{3.667} d\tau = 17510 \ Pa^3 s^{-1}$$

This agrees with the value found by numerical integration and would give the same value for u.

Note that the values of the apparent viscosity μ_0 were not used; they were provided to show that the fluid is strongly shear thinning. If the data were available as values of μ_0 at corresponding values of $\dot{\gamma}$, then τ should be calculated as their product. The table of values of $\tau^2\dot{\gamma}$ (Table 6) illustrates the fact that flow in the centre makes a small contribution to the total flow: flow in the outer parts of the pipe is most significant.

As mentioned previously, the minus sign in equation (17) reflects the fact that the shear rate is negative for flow in a pipe. In the above calculations, the absolute values of $\dot{\gamma}$, and τ have been used and the minus sign has therefore been dropped.

5. Wall shear stress-flow characteristic curves and scale-up for laminar flow

When data are available in the form of the flow rate-pressure gradient relationship obtained in a small diameter tube, direct scale-up for flow in larger pipes can be done. It is not necessary to determine the τ-$\dot{\gamma}$ curve with the true value of $\dot{\gamma}$ calculated from the

Rabinowitsch-Mooney equation (Equation (20)). Equation (17) shows that the flow characteristic is a unique function of the wall shear stress for a particular fluid:

$$\frac{8u}{D} = \frac{4}{\tau_w^3} \int_0^{\tau_w} \tau^2 (-\dot{\gamma}) d\tau$$

In the case of a Newtonian fluid, substituting $\dot{\gamma} = -\tau / \mu$ into the above equation and evaluating the integral gives

$$\frac{8u}{D} = \frac{\tau_w}{\mu} \tag{22}$$

Recall that the wall shear rate for a Newtonian fluid in laminar flow in a tube is equal to $-8u/D$. In the case of a non-Newtonian fluid in laminar flow, the flow characteristic is no longer equal to the magnitude of the wall shear rate. However, the flow characteristic is still related uniquely to τ_w because the value of the integral, and hence the right hand side of equation (17), is determined by the value of τ_w.

If the fluid flows in two pipes having internal diameters D_1 and D_2 with the same value of the wall shear stress in both pipes, then from equation (17) the values of the flow characteristic are equal in both pipes:

$$\frac{8u_1}{D_1} = \frac{8u_2}{D_2} \tag{23}$$

So the average velocities are related by

$$\frac{u_1}{u_2} = \frac{D_1}{D_2} \tag{24}$$

By substituting for u or by writing the flow characteristic as $-4Q/\pi R^3$, the volumetric flow rates are related by

$$\frac{Q_1}{Q_2} = \left(\frac{D_1}{D_2}\right)^3 \tag{25}$$

It is important to appreciate that the same value of τ_w requires different values of the pressure gradient in the two pipes. It is convenient to represent the flow behaviour as a graph of τ_w plotted against $8u/D$, as shown in Figure 3. In accordance with the above discussion, all data fit a single line for laminar flow. The graph is steeper for turbulent flow and different lines are found for different pipe diameters. It is noteworthy that the same would be found for Newtonian flow if the data were plotted in this way and the laminar flow line would be a straight line of gradient μ passing through the origin. The plot in Figure 3 is not a true flow curve because the flow characteristic is equal to the magnitude of the wall shear rate only in the case of Newtonian laminar flow.
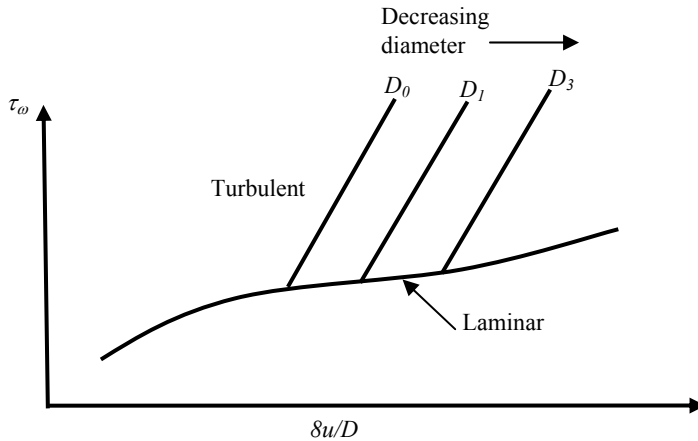
Fig. 3. Shear stress at the pipe wall against flow characteristic for a non-Newtonian fluid flowing in a pipe

Given a wall shear stress-flow characteristic curve such as that in Figure 3, the flow rate-pressure drop relationship can be found for any diameter of pipe provided the flow remains laminar and is within the range of the graph. For example, if it is required to calculate the pressure drop for flow in a pipe of given diameter at a specified volumetric flow rate, the value of the flow characteristic $(8u/D = 4Q/\pi R^3)$ is calculated and the corresponding value of the wall shear stress τ_w read from the graph. The pressure gradient, and hence the pressure drop for a given pipe length, can then be calculated.

It is found useful to define two quantifies K' and n' in order to describe the τ_w -flow characteristic curve. If the laminar flow data are plotted on logarithmic axes as in Figure 4, then the gradient of the curve defines the value of n' :

$$n' \;=\; \frac{d\ln \tau_w}{d\ln(8u/D)} \tag{26}$$

The equation of the tangent can be written as

$$\tau_w \;=\; K'\left(\frac{8u}{D}\right)^{n'} \tag{27}$$

In general, both K' and n' have different values at different points along the curve. The values should be found at the point corresponding to the required value of τ_w. In some cases, the curve in Figure 4 will be virtually straight over the range required and a single value may be used for each of K' and n'. Although equation (27) is similar to the equation of a power law fluid, the two must not be confused.

The reason for defining n' in this way can be seen from equation (21) where the inverse of the derivative occurs in the correction factor. Equation (20) can be written in terms of n' as
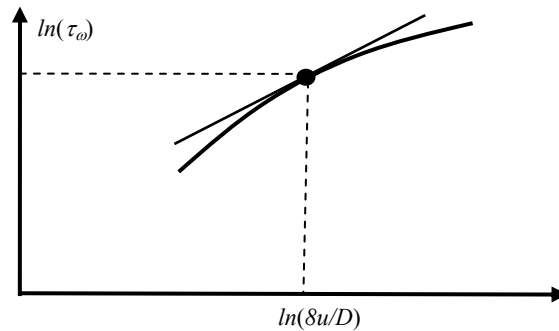
Fig. 4. Logarithmic plot of wall shear stress against flow characteristic: the gradient at a point defines n'

$$\dot{\gamma}_\omega \;=\; \dot{\gamma}_{\omega N}\left(\frac{3n'+1}{4n'}\right) \tag{28}$$

Equation (28) is helpful in showing how the value of the correction factor in the Rabinowitsch-Mooney equation corresponds to different types of flow behaviour. For a Newtonian fluid, n' = 1 and therefore the correction factor has the value unity. Shear thinning behaviour corresponds to n' < 1 and consequently the correction factor has values greater than unity, showing that the wall shear rate $\dot{\gamma}_w$ is of greater magnitude than the value for Newtonian flow. Similarly, for shear thickening behaviour, $\dot{\gamma}_w$ is of a smaller magnitude than the Newtonian value $\dot{\gamma}_{wN}$. The value correction factor varies from 2.0 for n' = 0.2 to 0.94 for n' = 1.3.

6. Generalized Reynolds number for flow in pipes

It is recalled that for Newtonian flow in a pipe, the Reynolds number is defined by

$$Re \;=\; \frac{\rho u D}{\mu} \tag{29}$$

In the case of non-Newtonian flow, it is necessary to use an appropriate apparent viscosity. Although the apparent viscosity μ_a is defined in the same way as for a Newtonian fluid, it no longer has the same fundamental significance and other, equally valid, definitions of apparent viscosities may be made. In flow in a pipe, where the shear stress varies with radial location, the value of μ_a varies. It is shown that the conditions near the pipe wall that are most important. The value of μ_a evaluated at the wall is given by

$$\mu_a \;=\; -\;\frac{\text{shear stress at wall}}{\text{shear rate at wall}} \;=\; \frac{\tau_\omega}{(-dv_x\,/\,dr)_\omega} \tag{30}$$

Another definition is based, not on the true shear rate at the wall, but on the flow characteristic. This quantity, which may be called the apparent viscosity for pipe flow, is given by

$$\mu_{ap} \ = \ \frac{\text{shear stress at wall}}{\text{flow characteristic}} = \frac{\tau_\omega}{(8u / d_i)} \tag{31}$$

For laminar flow, μ_{ap} has the property that it is the viscosity of a Newtonian fluid having the same flow characteristic as the non-Newtonian fluid when subjected to the same value of wall shear stress. In particular, this corresponds to the same volumetric flow rate for the same pressure gradient in the same pipe. This suggests that μ_{ap} might be a useful quantity for correlating flow rate-pressure gradient data for non-Newtonian flow in pipes. This is found to be the case and it is on μ_{ap} that a generalized Reynolds number Re' is based

$$\text{Re}' \ = \ \frac{\rho u d_i}{\mu_{ap}} \tag{32}$$

Representing the fluid's laminar flow behaviour in terms of K' and n'

$$\tau_\omega \ = \ K'\left(\frac{8u}{d_i}\right)^{n'} \tag{33}$$

The pipe flow apparent viscosity, defined by equation 31, is given by

$$\mu_{ap} \ = \ \frac{\tau_\omega}{8u / d_i} = K'\left(\frac{8u}{d_i}\right)^{n'-1} \tag{34}$$

Using μ_{ap} in Equation (34), the generalized Reynolds number takes the form

$$Re' \ = \ \frac{\rho u^{2-n'} d_i^{n'}}{8^{n'-1} K'} \tag{35}$$

Use of this generalized Reynolds number was suggested by Metzner and Reed (1955). For Newtonian behaviour, $K' = \mu$ and $n' = 1$ so that the generalized Reynolds number reduces to the normal Reynolds number.

7. Turbulent flow of Inelastic non-Newtonian fluids in pipes and circular ducts

Turbulent flow of Newtonian fluids is described in terms of the Fanning friction factor, which is correlated against the Reynolds number with the relative roughness of the pipe wall as a parameter. The same approach is adopted for non-Newtonian flow but the generalized Reynolds number is used. The Fanning friction factor is defined by

$$f \ = \ \frac{\tau_\omega}{\frac{1}{2}\rho u^2} \tag{36}$$

It is straightforward to show that the Fanning friction factor for laminar non-Newtonian flow becomes

$$f \ = 16 / \text{Re}' \tag{37}$$

This is of the same form as equation for Newtonian flow and is one reason or using this form of generalized Reynolds number. Equation (37) provides another way of calculating the pressure gradient for a given flow rate for laminar non-Newtonian flow.

7.1 Laminar-turbulent transition

A stability analysis made by Ryan and Johnson (1959) suggests that the transition from laminar to turbulent flow for inelastic non-Newtonian fluids occurs at a critical value of the generalized Reynolds number that depends on the value of n'. The results of this analysis are shown in Figure 5. This relationship has been tested for shear thinning and for Bingham plastic fluids and has been found to be accurate. Over the range of shear thinning behaviour encountered in practice, $0.2 \leq n' \leq 1$, the critical value of Re' is in the range $2100 \leq Re' \leq 2400$.
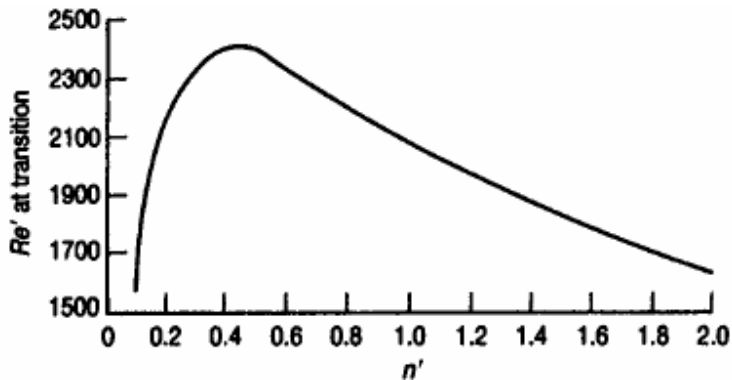
Fig. 5. Variation of the critical value of the Reynolds number with n'

7.2 Friction factors for turbulent flow in smooth pipes

Experimental results for the Fanning friction factor for turbulent flow of shear thinning fluids in smooth pipes have been correlated by Dodge and Metzner (1959) as a generalized form of the yon Kármán equation:

$$\frac{1}{f^{1/2}} = \frac{4.0}{(n')^{0.75}} \log[f^{1-n'/2} Re'] - \frac{0.40}{(n')^{1.2}}$$
(38)

This correlation is shown in Figure 6. The broken lines represent extrapolation of equation (38) for values of n' and Re' beyond those of the measurements made by Dodge and Metzner. More recent studies tend to confirm the findings of Dodge and Metzner but do not significantly extend the range of applicability. Having determined the value of the friction factor f for a specified flow rate and hence Re', the pressure gradient can be calculated in the normal way.

Example 3

A general time-independent non-Newtonian liquid of density 961 kg/m³ flows steadily with an average velocity of 2.0*m/s* through a tube 3.048 m long with an inside diameter of 0.0762 m. For these conditions, the pipe flow consistency coefficient K' has a value of 1.48 Pa s[0.3]

and n' a value of 0.3. Calculate the values of the apparent viscosity for pipe flow μ_{ap}, the generalized Reynolds number Re' and the pressure drop across the tube, neglecting end effects.
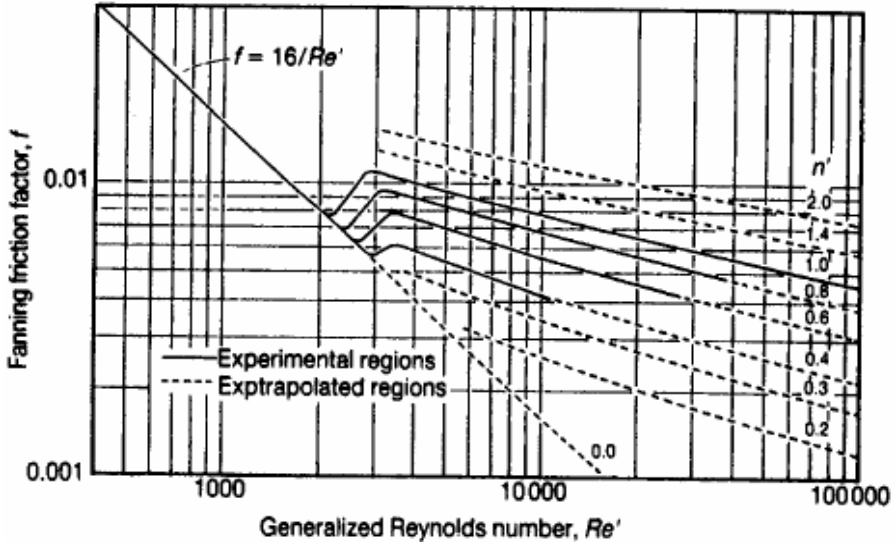
Source: D. W. Dodge and A. B. Metzner, *AIChE Journal* **5** (1959) 189-204

Fig. 6. Friction factor chart for purely viscous non-Newtonian fluids.

Calculations

The flow characteristic is given by

$$\frac{8u}{D} = \frac{8(2.0m/s)}{0.0762m} = 210s^{-1}$$

and

$$\left(\frac{8u}{D}\right)^{n'-1} = 210^{(0.3-1.0)} = 0.0237s^{0.7}$$

Hence

$$\mu_{ap} = K'\left(\frac{8u}{D}\right)^{n'-1} = (1.48 \text{ Pa s}^{0.3})(0.0237 \text{ } s^{0.7}) = 0.0351 \text{ Pa s}$$

and

$$Re' = \frac{\rho u D}{\mu_{ap}} = \frac{(0.0762 \text{ m})(2.0 \text{ m})(961 \text{ kg/m}^3)}{(0.0351 \text{ Pa s})} = 4178$$

From Figure 6, the Fanning friction factor *f* has a value 0.0047. Therefore the pressure drop is given by

$$\Delta P_f \;=\; 4f\left(\frac{L}{d_i}\right)\frac{\rho \mathrm{u}^2}{2} = \; \frac{2(0.0047)(3.048 \text{ m})(961 \text{ kg/m}^3)(2.0 \text{ m/s})^2}{(0.0762 \text{ m})} = 1445 \text{ Pa}$$

8. Laminar flow of inelastic fluids in non-circular ducts

Analytical solutions for the laminar flow of time-independent fluids in non-axisymmetric conduits are not possible. Numerous workers have obtained approximate and/or complete numerical solutions for specific flow geometries including square, rectangular and triangular pipes (Schechter, 1961 ; Wheeler and Wissler, 1965 ; Miller, 1972 ; Mitsuishi and Aoyagi, 1969, 1973). On the other hand, semi-empirical attempts have also been made to develop methods for predicting pressure drop for time-independent fluids in ducts of non-circular cross-section. Perhaps the most systematic and successful friction factor analysis is that provided by Kozicki *et al* . (1966, 1967) . It is useful to recall here that the equation (19) is a generalized equation for the laminar flow of time-independent fluids in a tube and it can be slightly rearranged as:

$$-\dot{\gamma}_w = f(\tau_w) = \frac{1}{4}\tau_w \frac{d(8u/D)}{d\tau_w} + \frac{3}{4}(\frac{8u}{D}) \tag{39}$$

Similarly, one can parallel this approach for the fully developed laminar flow of time independent fluids in a thin slit (Figure 7) to derive the following relationship:

$$-\dot{\gamma}_w = \left(-\frac{dV_z}{dr}\right)_w = f(\tau_w) = \tau_w \frac{d(u/h)}{d\tau_w} + 2(\frac{u}{h}) \tag{40}$$

In order to develop a unified treatment for ducts of various cross-sections, it is convenient to introduce the usual hydraulic diameter D_h (defined as four times the area for flow/wetted perimeter) into equations (39) and 40).

For a circular pipe, $D_h = D$ and hence equation (38) becomes:

$$-\dot{\gamma}_\omega = f(\tau_\omega) = \frac{1}{4}\tau_\omega \frac{d(8u/D_h)}{d\tau_\omega} + \frac{3}{4}(\frac{8u}{D_h}) \tag{41}$$

For the slit shown in Figure 7, the hydraulic diameter $D_h = 4h$, and thus equation (39) is rewritten as:

$$-\dot{\gamma}_w = = \frac{1}{2}\tau_w \frac{d(8u/D_h)}{d\tau_w} + (\frac{8u}{D_h}) \tag{42}$$

By noting the similarity between the form of the Rabinowitsch–Mooney equations for the flow of time-independent fluids in circular pipes (equation (41)) and that in between two plates (equation (42)), they suggested that it could be extended to the ducts having a constant cross-section of arbitrary shape as follows:

$$-\dot{\gamma}_w = f(\overline{\tau}_w) = a\overline{\tau}_w \frac{d(8u/D_h)}{d\overline{\tau}_w} + b(\frac{8u}{D_h})$$ (43)
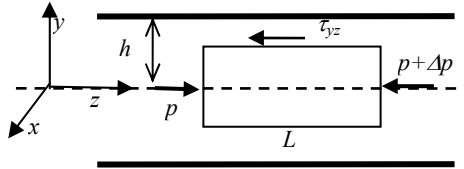

Fig. 7. Laminar flow between parallel plates

where a and b are two geometric parameters characterizing the cross-section of the duct ($a=1/4$ and $b=3/4$ for a circular tube, and $a=1/2$ and $b=1$ for the slit) and $\overline{\tau}_w$ is the mean value of shear stress at the wall, and is related to the pressure gradient as:

$$\overline{\tau}_w = \frac{D_h}{4}\left(\frac{-\Delta P}{L}\right)$$ (44)

For constant values of a and b, equation (42) is an ordinary differential equation of the form $(dy/dx) + p(x)y = q(x)$ which can be integrated to obtain the solution as:

$$y = e^{-\int p(x)dx} \int e^{\int p(x)dx} q(x)dx + C_0$$ (45)

Now identifying $y = (8V/D_h)$ and $x = \overline{\tau}_w$, $p(x) = (b/a\overline{\tau}_w)$ and $q(x) = (f(\overline{\tau}_w)/a\overline{\tau}_w)$, the solution to equation (43) is given as:

$$\frac{8u}{D_h} = \frac{1}{a}(\overline{\tau}_w)^{-b/a} \int_0^{\overline{\tau}_w} \xi^{(b/a)-1} f(\tau)d\xi$$ (46)

where ξ is a dummy variable of integration. The constant C_0 has been evaluated by using the condition that when $V=0$, $\overline{\tau}_w = 0$ and therefore, $C_0 = 0$.

For the flow of a power-law fluid, $f(\tau) = (\tau/K)^{1/n}$ and integration of equation (46) yields:

$$\overline{\tau}_w = K\left\{\frac{8u}{D_n}(b+\frac{a}{n})\right\}^n$$ (47)

which can be rewritten in terms of the friction factor, $f = 2\overline{\tau}_w/\rho u^2$ as:

$$f = \frac{16}{Re_g}$$ (48)

where the generalized Reynolds number,

$$Re_g = \frac{\rho u^{2-n}D_h^n}{8^{n-1}K(b+\frac{a}{n})^n}$$ (49)

| 1. *Concentric annuli*			
$\sigma = Ri/Ro$	a	b	
0.00	0.2500	0.7500	
0.01	0.3768	0.8751	
0.03	0.4056	0.9085	
0.05	0.4217	0.9263	
0.10	0.4455	0.9510	
0.20	0.4693	0.9737	
0.30	0.4817	0.9847	
0.40	0.4890	0.9911	
0.50	0.4935	0.9946	
0.80	0.4992	0.9994	
1.00	0.5000	1.0000	
2. *Elliptical ducts*			
$\varepsilon = b'/a'$	a	b	
0.00	0.3084	0.9253	
0.10	0.3018	0.9053	
0.20	0.2907	0.8720	
0.30	0.2796	0.8389	
0.40	0.2702	0.8107	
0.50	0.2629	0.7886	
0.60	0.2575	0.7725	
0.80	0.2515	0.7546	
1.00	0.2500	0.7500	
3. *Rectangular ducts*			
$e = H/W$	a	b	
0.00	0.5000	1.0000	
0.25	0.3212	0.8182	
0.50	0.2440	0.7276	
0.75	0.2178	0.6866	
1.00	0.2121	0.6766	
4. *Isosceles triangular ducts*			
$2a$	a	b	
10°	0.1547	0.6278	
20°	0.1693	0.6332	
40°	0.1840	0.6422	
60°	0.1875	0.6462	
80°	0.1849	0.6438	
90°	0.1830	0.6395	
5. *Regular polygonal ducts*			
N	a	b	
4	0.2121	0.6771	
5	0.2245	0.6966	
6	0.2316	0.7092	
8	0.2391	0.7241	
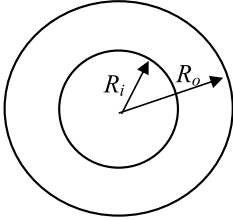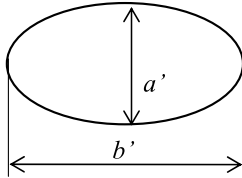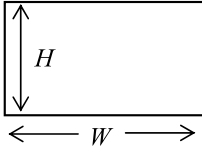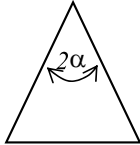
Table 7. Values of a and b depending on geometry of the ducts

The main virtue of this approach lies in its simplicity and the fact that the geometric parameters a and b can be deduced from the behaviour of Newtonian fluids in the same flow geometry. Table 7 lists values of a and b for a range of flow geometries commonly encountered in process applications.

Kozicki $et\ al.$(1966) argued that the friction factor of the turbulent flow in non-circular ducts can be calculated from the following equation

$$\frac{1}{\sqrt{f}} = \frac{4}{n^{0.75}} \log_{10}(\text{Re}_g\, f^{(2-n)/2}) - \frac{0.4}{n^{1.2}} + 4n^{0.25} \log[\frac{a(a+bn)}{3n+1}]$$ (50)

Note that since for a circular tube, a= 1/4 and b =3/4, equation (50) is consistent with that for circular pipes. The limited data available on turbulent flow in triangular (Irvine Jr, 1988), rectangular (Kostic and Hartnett, 1984) and square ducts (Escudier and Smith, 2001) conforms to equation (48). In the absence of any definite information, Kozicki and Tiu (1988) suggested that the Dodge–Metzner criterion, $Re_g \leq 2100$, can be used for predicting the limit of laminar flow in non-circular ducts.

Some further attempts have been made to simplify and/or improve upon the two geometric parameter method of Kozicki $et\ al$. (1966, 1967). Delplace and Leuliet (1995) revisited the definition of the generalized Reynolds number (equation (49)) and argued that while the use of a and b accounts for the non-circular cross-sections of the ducts, but the factor 8^{n-1} appearing in the denominator is strictly applicable for the flow in circular ducts only. Their reasoning hinges on the fact that for the laminar flow of a Newtonian fluid, the product ($f.Re$) is a function of the conduit shape only. Thus, they wrote

$$\beta = \frac{48}{(f.Re)}$$ (51)

where both the (Fanning) friction factor and the Reynolds number are based on the use of the hydraulic diameter, D_h and the mean velocity of the flow, u. Furthermore, they were able to link the geometric parameters a and b with the new parameter β as follows:

$$a = \frac{1}{1+\beta}; \quad b = \frac{\beta}{1+\beta}$$ (52)

and finally, the factor of 8^{n-1} in the denominator in equation (49) is replaced $(24/\beta)^{n-1}$. With these modifications, one can use the relationship $f = (16/Re_g)$ to estimate the pressure gradient for the laminar flow of a power-law fluid in a non-circular duct for which the value of β is known either from experiments or from numerical results. Therefore, this approach necessitates the knowledge of only one parameter (β) as opposed to the two geometric parameters, namely, a and b in the method of Kozicki $et\ al$. (1966) and Kozicki and Tiu (1967), albeit a similar suggestion was also made by Miller (1972) and Liu (1983). Finally, for the limiting case of a circular pipe, evidently β=3 thereby leading to a=(1/4) and b=(3/4) and the two definitions of the Reynolds number coincide, as expected. The values of β for a few standard duct shapes are summarized in Table 5. While in laminar flow, these two methods give almost identical predictions, the applicability of the modified method of Delplace and Leuliet (1995) has not been checked in the transitional and turbulent flow regions. Scant

analytical and experimental results suggest that visco-elasticity in a fluid may induce secondary motion in non-circular conduits, even under laminar conditions. However, measurements reported to date indicate that the friction factor–Reynolds number behaviour is little influenced by such secondary flows (Hartnett and Kostic, 1989).

Example 4

A power-law fluid (K = 0.3 Pa.s^n and n = 0.72) of density 1000 kg/m^3 is flowing in a series of ducts of the same flow area but different cross-sections as listed below:

i.   concentric annulus with R= 37mm and $\sigma=(R/R_i)$= 0.40
ii. circular pipe of radius R
iii. rectangular, (H/W) =0.5
iv. elliptical, b'/a' = 0.5

Estimate the pressure gradient required to maintain an average velocity of 1.25m/s in each of these channels. Use the geometric parameter method. Also, calculate the value of the generalized Reynolds number as a guide to the nature of the flow.

Solution

i.   For a concentric annulus, σ = 0.4

-    From Table 6 we have: a =0.489; b = 0.991
-    The hydraulic diameter, D_h = $2R(1-\sigma)$=0.044m.

-    Reynolds number, $\mathrm{Re}_g = \dfrac{\rho u^{2-n} D_h^n}{8^{n-1} K (b+\dfrac{a}{n})^n} = 579$

-    Thus, the flow is laminar and the friction factor is estimated as: f=1/578=0.0276 and

$$-\frac{\Delta P}{L} = \frac{2 f \rho u^2}{D_h} = 1963 \, Pa/m$$

ii. For a circular tube, the area of flow

-    For a circular pipe, a =0.25, b = 0.75, D_h = D = 0.0678m

-    Reynolds number, $\mathrm{Re}_g = \dfrac{\rho u^{2-n} D_h^n}{8^{n-1} K (b+\dfrac{a}{n})^n} = 1070$

-    The flow is laminar and the friction factor is estimated as: f=1/1070=0.01495 and

$$-\frac{\Delta P}{L} = \frac{2 f \rho u^2}{D_h} = 689 \, Pa/m$$

iii. For a rectangular duct with H/W = 0.5, H =0.0425 m and W= 0.085 m (for the same area of flow), and from Table 6: a=0.244, b= 0.728

-    D_h = 4HW/2(H+W) = 0.0567m

-    Reynolds number, $\mathrm{Re}_g = \dfrac{\rho u^{2-n} D_h^n}{8^{n-1} K (b+\dfrac{a}{n})^n} = 960$

- f=1/960=0.0167 and $-\dfrac{\Delta P}{L} = \dfrac{2f\rho u^2}{D_h} = 919 Pa/m$

iv. elliptical, $b'/a' = 0.5$.

- From Table 6 : a=0.2629, b= 0.7886
- D_h = = $0.0607m$
- Reynolds number, $\text{Re}_g = 953$

- f =0.0168 and $-\dfrac{\Delta P}{L} = 864 Pa/m$

9. References

Astarita, G., The Engineering Reality of the Yield Stress, *J. Rheol.* 34 (1990) 275

Barnes , H.A. and Walters , K. , The yield stress myth, *Rheol. Acta* 24 (1985) 323 .

Barnes , H.A. , Edwards , M.F. and Woodcock , L.V. , Applications of computer simulations to dense suspension rheology, *Chem. Eng. Sci.* 42 (1987) 591 .

Barnes , H.A. , Hutton , J.F. and Walters , K. , An Introduction to Rheology , *Elsevier*, Amsterdam (1989) .

Barnes , H.A., The yield stress - a review, *J. Non-Newt. Fluid Mech.* 81 (1999) 133.

Bird , R.B. , Useful non-Newtonian models, *Annu. Rev. Fluid Mech.* 8 (1976) 13.

Bird , R.B. , Dai , G.C. and Yarusso , B.J. , The rheology and flow of viscoplastic materials, *Rev. Chem. Eng.* 1 (1983) 1 .

Bird , R.B. , Armstrong , R.C. and Hassager , O. , Dynamics of polymeric liquids. Fluid dynamics, 2nd edition, Wiley , New York (1987) .

Cross , M.M. , Rheology of non-Newtonian fluids: A new flow equation for pseudoplastic systems*, J. Colloid Sci.* 20 (1965) 417.

Carreau , P.J. , Rheological equations from molecular network theories, *Trans. Soc. Rheol.* 16 (1972) 99.

Carreau , P.J. , Dekee , D. and Chhabra , R.P., Rheology of polymeric systems: Principles and applications , (1997)

Delplace , F. and Leuliet , J. C. , Generalized Reynolds number for the flow of power law fluids in cylindrical ducts of arbitrary cross-section, Chem. Eng. Journal, 56, 33-37., *Chem. Eng. J.* 56 (1995) 33.

Dodge, D. W. and Metzner, A. B., Turbulent flow of non-Newtonian systems, *AIChE Journal.* 5 (1959) 189-204.

Escudier , M.P. and Smith , S. , Non-Newtonian liquids through a square duct, *Proc. Royal Soc.* 457 (2001) 911 .

Evans , I. D. , On the nature of the yield stress, *J. Rheol.* 36 (1992) 1313 .

Goddard , J.D. and Bashir , Y. , Recent developments in structured continua II (Chapter 2) , Longman , London (1990) .

Griskey, R.G., Nechrebecki, D.G., Notheis , P.J. and Balmer , R.T., Rheological and pipeline flow dehavior of corn starch dispersions, *J. Rheol.* 29(1985) 349

Hartnett , J.P. and Kostic , M. , Heat transfer to Newtonian and non- Newtonian fluids in rectangular duct, *Adv. Heat Transf.* 19 (1989) 247.

Irvine , Jr. , T.F. , A generalized blasius equation for power law liquids, *Chem. Eng. Commun.* 65 (1988) 39.

Johnson , A.T. , Biological Process Engineering , Wiley , New York (1999).

Kozicki , W. , Chou , C.H. and Tiu , C. , Non-Newtonian flow in ducts of arbitrary cross-sectional shape, *Chem. Eng. Sci.* 21 (1966) 665 .

Kozicki , W. , and Tiu , C., Non-Newtonian flow through open channels, *Chem. Eng.* 45 (1967) 127 .

Kozicki , W. and Tiu , C. , Encyclopedia of Fluid Mechanics, Vol. 7, Gulf, Houston , p. 199 (1988).

Kostic , M. and Hartnett , J.P. , Predicting turbulent friction factors of non- Newtonian fluids in noncircular ducts, *Int. Comm. Heat Mass Transf.* 11 (1984) 345 .

Metzner , A.B. and Whitlock , M. , Flow behavior of concentrated (dilatant) suspensions, *Trans. Soc. Rheol.* 2 (1958) 239 .

Metzner, A.B. and Reed, J.C., Flow of non-Newtonian fluids correlation of the laminar, transition, and turbulent-flow regimes, *AIChE Journal*. 1 (1955) 434-40.

Miller , C. , Predicting non-Newtonian flow behaviour in ducts of unusual cross-sections *Ind. Eng. Chem. Fundam.* 11 (1972) 524 .

Mitsuishi , N. and Aoyagi , Y. , Non-Newtonian flow in non- circular ducts, *Chem. Eng. Sci .* 24 (1969) 309 .

Mitsuishi , N. and Aoyagi , Y. , Non-Newtonian fluid flow in an eccentric annulus, *J. Chem. Eng. Jpn.* 6 (1973) 402 .

Ryan, N.W. and Johnson, M.M., Transition from laminar to turbulent flow in pipes, *AIChE Journal*. 5 (1959) 433.

Schechter, R.S. , On the steady flow of a non-Newtonian fluid in cylinder ducts, *AIChE J.* 7 (1961) 445 .

Schurz , J. , The yield stress - an empirical reality, *Rheol. Acta.* 29 (1990) 170 .

Uhlherr , P.H.T. , Guo , J. , Zhang , X-M. , Zhou , J.Z and Tiu , C. , The shear-induced solid-liquid transition in yield stress materials with chemically different structures, *J. Non-Newt. Fluid Mech.* 125 (2005) 101 .

Wheeler , J.A. and Wissler , E.H. , The Friction factor-Reynolds number relation for a steady flow of pseudoplastic fluids through rectangular ducts, *AIChE J.* 11 (1965) 207.
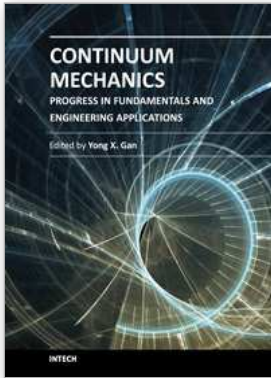
Continuum Mechanics - Progress in Fundamentals and Engineering Applications
Edited by Dr. Yong Gan

Continuum Mechanics is the foundation for Applied Mechanics. There are numerous books on Continuum Mechanics with the main focus on the macroscale mechanical behavior of materials. Unlike classical Continuum Mechanics books, this book summarizes the advances of Continuum Mechanics in several defined areas. Emphasis is placed on the application aspect. The applications described in the book cover energy materials and systems (fuel cell materials and electrodes), materials removal, and mechanical response/deformation of structural components including plates, pipelines etc. Researchers from different fields should be benefited from reading the mechanics approached to real engineering problems.

How to reference
In order to correctly reference this scholarly work, feel free to copy and paste the following:

INTECH
open science | open minds